Liquid Crystals
Publication details, including instructions for authors and subscription information:
http://www.informaworld.com/smpp/title~content=t713926090

Proton NMR investigation of a hydrogen-bonded liquid crystal gel

Jianjun Li Corresponding author[a]; Dieter Geschke[a]; Ralf Stannarius[b]
[a] University of Leipzig, Institute of Experimental Physics I, D-04103 Leipzig, Germany [b] University of Magdeburg, Institute of Experimental Physics, D-39106 Magdeburg

To cite this Article Li Corresponding author, Jianjun , Geschke, Dieter and Stannarius, Ralf(2004) 'Proton NMR investigation of a hydrogen-bonded liquid crystal gel', Liquid Crystals, 31: 1, 21 — 29
To link to this Article: DOI: 10.1080/02678290310001628483
URL: http://dx.doi.org/10.1080/02678290310001628483

LIQUID CRYSTALS, VOL. 31, NO. 1, JANUARY 2004, 21–29

Proton NMR investigation of a hydrogen-bonded liquid crystal gel

JIANJUN LI*, DIETER GESCHKE
University of Leipzig, Institute of Experimental Physics I, Linnéstrasse 5,
D-04103 Leipzig, Germany

and RALF STANNARIUS
University of Magdeburg, Institute of Experimental Physics, Universitätsplatz 2,
D-39106 Magdeburg

(*Received 29 May 2003; accepted 27 August 2003*)

Proton NMR is employed to determine director distributions in a hydrogen-bonded liquid crystal gel in the presence of a magnetic field. The samples consist of the mesogen 8CB mixed with small percentages of gelator, which forms a hydrogen-bonded network when the sample is cooled below the gelation point in the isotropic liquid. Since the gelation occurs above the clearing point, a non-oriented random director configuration is frozen in. The configuration of the hydrogen-bonded network is found to be isotropic. It fixes a preferential random local orientation of the nematic director, even in the presence of an external magnetic field of a few Tesla. The NMR spectra of the samples give information on orientation and order in such systems. A simple model for the director field is provided.

1. Introduction

Liquid crystal (LC) gels [1] have attracted increasing interest over the past decade. This has been initiated not only by fundamental scientific questions but also by the potential for applications, such as reflective displays based on the polymer network stabilized cholesteric texture, or in the enhancement of the mechanical stability of ferroelectric LC displays [2]. It has been shown that the formation of a network by the chemical crosslinking of a few percent of photoreactive additives in a low molar mass mesogenic material can stabilize the orientation of the mesogens. This leads to dramatic changes in the dynamics and the electro-optic characteristics [1, 2]. Besides the electro-optical effects connected with the mesogenic properties, interactions of the gel network with the orientational order of the mesogens lead to a coupling of macroscopic sample sizes and shapes to the microscopic order and may influence, for example, the swelling characteristics of anisotropic gels [3].

Recently, scientific attention has focused also on the *physical* gelation of organic solvents by the fibrous aggregation of small molecules (gelator) in a thermotropic liquid crystal environment [4–14]. Self-assembly and micrometer scale phase segregation of these two discrete components, i.e. the hydrogen-bonded gelators and the conventional rodlike LC molecules, results in the generation of physical LC gels [4, 5]. The fibrous network aggregates in the liquid crystal and causes the formation of an anisotropic soft solid. The physical network formed by the gelators can stabilize the orientational state of LC phases [11, 12]. In turn, the orientational state of the mesogens may influence the topology of the network structure (e.g. [4, 10, 12]). In contrast to chemically crosslinked gels, the network formation is completely thermo-reversible. In particular, LC physical gels have shown very promising application potential in twisted nematic cells if a suitable concentration of the gelators is chosen. This type of physical nematic gel seems to show advantages for light-scattering electro-optical materials, which may lead to the fabrication of thin, flexible LC-based displays [4, 8, 9, 14]. However, relatively little is known about the stabilizing effects of such hydrogen-bonded ('physical') gel networks on the director orientation in external electromagnetic fields.

Proton and deuterium nuclear magnetic resonance (NMR) spectroscopies have proved to be powerful methods for the investigation of nematic structures in the bulk and in micrometer confined samples [15–17]. NMR spectroscopy is used here to obtain information on the director distributions in nematic gel samples. We have prepared cells with different concentrations of gelators and measured the state of orientation of the nematic director by proton NMR. These first NMR

*Author for correspondence; e-mail: jjli@rz.uni-leipzig.de

Liquid Crystals ISSN 0267-8292 print/ISSN 1366-5855 online © 2004 Taylor & Francis Ltd
http://www.tandf.co.uk/journals
DOI: 10.1080/02678290310001628483

experiments on such physical LC gels demonstrate that NMR provides straightforward access to the director distribution in these systems. It is shown that above a certain concentration of the gelling agent, the random director alignment frozen in by the network during gelation in the isotropic phase is stable in the magnetic field.

2. Theoretical

Although the information obtained from ^{2}H NMR spectra of partially deuterated samples is more detailed than that provided by proton NMR, the latter technique has certain advantages because it can be applied without the need to prepare the deuteriated material. Proton NMR also has the advantage of high sensitivity, which is of special importance in the investigation of thin layers.

The complex ^{1}H NMR line shape is determined by the interactions between all ^{1}H nuclei in the material, and is primarily of dipolar origin. The NMR resonance line for the simplest case of a two-proton system is a doublet according to the two orientations of the proton spin in the $\mathbf{B}_0$ field. The dipolar splitting frequency is given by a constant prefactor

$$\frac{3\mu_0}{16\pi^2}\frac{\gamma^2\hbar}{\langle r^3\rangle}$$

(with the mean cubic proton–proton distance $\langle r^3\rangle$, the proton gyromagnetic ratio γ, the vacuum permeability μ_0 and Planck's constant divided by 2π, $\hbar$), and by an angular dependent factor that describes the time-averaged orientation of the proton–proton interconnection vector with respect to the magnetic field. This orientational dependence can be calculated, given the assumption that intramolecular motions and molecular dynamics are independent of each other, using three factors: a conformation tensor, which accounts for the molecular geometry and time-averaged orientation of the proton–proton interconnection vector in the molecular frame; the fourth rank nematic order tensor which describes the ensemble-averaged orientation of the molecular frame in the director frame; and an additional scalar factor $S_\theta=(3\cos^2\theta-1)/2$ giving the orientation of the spectrometer magnetic field $\mathbf{B}_0$ with respect to the director (θ denotes the angle between the magnetic field and local director).

For the uniaxial nematic phase, the order tensor which describes the averaged orientation of a molecule-fixed coordinate system with respect to the director reduces to two non-zero independent elements S^{cc}_{zz}, and $S^{aa}_{zz}-S^{bb}_{zz}$, where z is the coordinate along the director and a, b, c are the axes of a coordinate system fixed to the molecular core. Here, c is assigned to the molecular long axis which deviates only by a few degrees from the *para*-axes of the core benzene units. The order tensor element $S=S^{cc}_{zz}=\langle 3(\cos^2\vartheta-1)/2\rangle$ is the conventional nematic order parameter (with ϑ the angle between the director and the molecular long axis c and $\langle\rangle$ the average taken over the ensemble of molecules). The only other remaining non-zero element of the order tensor, $D=S^{aa}_{zz}-S^{bb}_{zz}$, is usually very small ($<10\%$ of S) and thus may be neglected. All dipolar interactions are time-averaged by fast molecular motions and projected on the molecular long axis c. Due to the resulting dependence of all averaged dipolar interactions on the order parameter S, and the orientation of the director with respect to the magnetic field $\mathbf{B}_0$ (included in S_θ), the line shape $f_\theta(\nu)$ of a domain with order parameter S in orientation θ to the magnetic field scales with

$$f_\theta(\nu)=\frac{1}{S_\theta S}f_0\left(\frac{\nu}{S_\theta S}\right). \qquad (1)$$

The spectral line shape $f_0(\nu)$ corresponds to the completely aligned sample when the order parameter S is extrapolated to 1. Here, we have assumed that the dipolar interactions give the dominant contributions to the Hamiltonian. Additional influences on the line shape arising from the different chemical shifts of chain (aliphatic) and ring (aromatic) protons are small compared with the dipolar interactions, except for domains in the vicinity of the magic angle ($S_\theta=0$) and in the isotropic phase ($S=0$), where the dipolar interactions vanish. *J*-couplings can also be neglected when compared with the other interactions. Since the direct calculation of the proton lineshape $f_\theta(\nu)$ from the molecular geometry requires considerable effort [18–20], we use instead a measured spectrum of the aligned nematic phase ($S_\theta=1$) of the pure compound to determine $f_0(\nu)$. Given some simplifying assumptions, it is possible to find the absolute order parameter scale from the oriented spectrum: the *ortho*-protons of the benzene ring are sufficiently isolated from the aliphatic chain protons, and the assumption of a predominantly pairwise interaction between neighbouring *ortho*-protons is rather good. In the proton NMR spectrum, their contributions appear as the dominant splitting in the spectrum (the additional shoulders can be assigned to the protons of the aliphatic chain segments near the ring). The direction of the proton–proton interconnection of the *ortho*-protons in the aromatic core is almost parallel to the molecular long axis c (in fact, the deviation is only of the order of 10°). Then, the splitting $\Delta\nu$ of an individual *ortho*-ring proton doublet is approximately

$$\Delta\nu=\frac{3\mu_0}{16\pi^2}\frac{\gamma^2\hbar}{\langle r^3\rangle}S_\theta S. \qquad (2)$$

Using known values for the *ortho*-proton distance, the prefactor gives $\nu_0 \cong 25.4\,\text{kHz}$. Therefore, the order parameter S of the core can be obtained from the dipolar splitting of the corresponding shoulders of the line shape of a well aligned sample:

$$\Delta\nu(S) = \nu_0\, S. \tag{3}$$

This equation is relevant only for the absolute scaling of the order parameter extracted from the spectrum. It plays no role in the analysis of the line shape regarding *relative* changes of the order parameter or the distribution function $n(\theta)$ of the director with respect to the field in a multidomain sample.

If the director is in an orientation perpendicular to the field, ($\theta = 90°$, $S_\theta = -1/2$), then the *ortho*-proton doublet splitting $\Delta\nu$ reduces to one half of the splitting of the aligned sample (and the overall spectral width is also reduced). At the magic angle $\theta_{\text{mag}} = 54.7°$, the dipolar splitting vanishes. Then, the line is very narrow and it is governed by the splitting due to the different chemical shifts of individual protons.

In a non-perfectly aligned, multi-domain sample, the NMR spectral line shape yields information about both the order parameter and the orientation of the molecules with respect to the $\mathbf{B}_0$ field. However, one has to make certain assumptions about this distribution since only the factor $S_\theta \cdot S$ appears in equation (1). The orientational distribution density of the director in the sample, $\tilde{n}(\theta, \varphi)$, (where φ is the azimuthal angle of the director with respect to $\mathbf{B}_0$) is unknown, and in general it cannot be derived completely from the NMR spectra without model-based assumptions, because only the angle θ influences the line shape:

$$F(\nu) = \frac{1}{4\pi}\int_0^{2\pi}\int_0^{\pi} f_\theta(\nu)\tilde{n}(\theta, \varphi)\sin\theta\, d\theta\, d\varphi. \tag{4}$$

Thus we introduce the quantity $n(\theta)$ which is obtained by integrating $\tilde{n}(\theta, \varphi)$ over the azimuthal angle

$$n(\theta) = \frac{2}{4\pi}\int_0^{2\pi} \tilde{n}(\theta, \varphi)\sin\theta\, d\varphi$$

(the additional factor of 2 accounts for the symmetry $n \leftrightarrow -n$). If the director distribution is cylindrically symmetric with respect to the field (for example, in powder samples or for all other situations where only $\mathbf{B}_0$ aligns the director), then $n(\theta)$ relates to $\tilde{n}(\theta)$ as $n(\theta) = \sin(\theta)\tilde{n}(\theta)$. Consequently, $n(\theta)$ approaches zero for $\theta = 0$, and for a random powder pattern $n(\theta) = \sin\theta$. With this 'polar angle distribution density' $n(\theta)$ of the director orientation with respect to $\mathbf{B}_0$, the line shape $F(\nu)$ is given by

$$F(\nu) = \int_0^{\pi/2} f_\theta(\nu)n(\theta)d\theta. \tag{5}$$

This line shape simulation is performed with a computer program that replaces the integral in equation (5) by the sum

$$F(\nu) = \frac{2}{\pi}\sum_{i=0}^{N-1} f_{\theta_i}(\nu)n(\theta_i)\Delta\theta,\ \theta_i = \left(i + \frac{1}{2}\right)\Delta\theta,\ \Delta\theta = \frac{\pi}{2N} \tag{6}$$

where N is chosen to be sufficiently large (≈ 100). This allows the calculation of the proton line shape from a given order parameter S and distribution density $n(\theta)$ of the director field.

3. Experimental

The chemical structures of the gelator and the low molar mass liquid crystal 8CB (Cr 21.5°C smectic A 33.5°C nematic 40.5°C isotropic) used in the experiments are presented in figure 1. The synthesis of the gelator is described in [11]. When the gel former is added in small quantities of a few percent (less than 5.0%, all percentages are given in wt%) to the mesogen, it is completely soluble and the mesomorphism is preserved, except for slight changes in the phase transition temperatures. Under a polarizing microscope, the gelling temperature in the system is determined to be 50°C, i.e. in the isotropic phase of 8CB (see next section). The gelator concentrations used here are high compared with other investigations of hydrogen-bonded LC gels (cf. [4, 8, 9, 13]). It is established that gelation using the same gel former occurs at lower concentrations than those studied here, see, for example FTIR investigations in a smectic

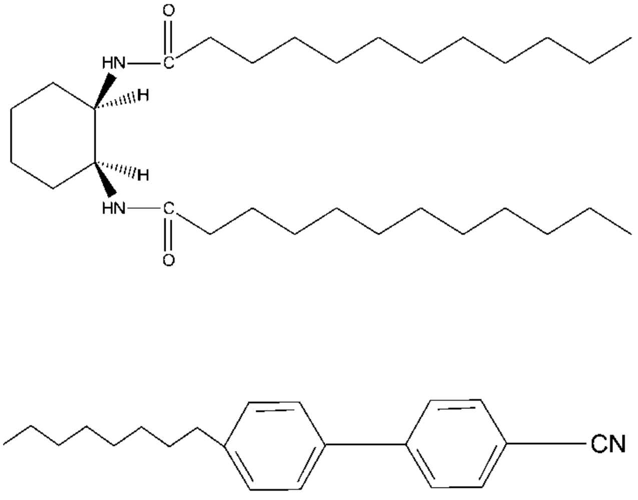

Figure 1. Chemical structures of gelling agent and mesogen used in the experiments.

material [13], but there is no effective stabilization of the director field in the comparably high NMR magnetic fields for low concentration samples, as will be shown later.

The 8CB and gel former mixture is contained in a sandwich cell made from indium tin oxide (ITO)-coated glass sheets separated by polyimide spacers. The glass surfaces were cleaned but not further treated. The cell thickness is about 100 µm, in order to achieve a sufficient sample signal. The cell was filled by capillary action, while the sample was kept 20 K above the clearing point for several minutes. For the NMR studies, it would of course be advantageous to use conventional sample tubes because of the larger sample size and better field homogeneity. However, in order to study the samples by polarizing microscopy as well as to preserve the option to apply electric fields in subsequent experiments in the same geometry, the sandwich geometry was preferred. The proton NMR signal is large enough in these samples, no intensity problems arise, and field homogeneity is not critical in the broad dipolar spectra. The cell thickness is still much larger than the internal structure of the gel network and the magnetic coherence length, so that boundary effects can be neglected. The texture and optics of the samples were investigated under a transmission microscope with crossed polarizers before and after the NMR measurements. All images were recorded with a Nikon Coolpix 990 CCD camera. The NMR spectra were obtained with a Bruker MSL 100 spectrometer working at a magnetic field of 2.34 T (100 MHz frequency for protons). The spectra were obtained by Fourier transformation of the FID recorded after a π/2 pulse. The length of the π/2 pulse is approximately 2.5 µs. The sample temperature was controlled with an accuracy better than 0.5 K. Up to 500 scans were accumulated for each spectrum to achieve a good signal-to-noise ratio. The angular dependence of the NMR spectra was measured by rotating the cell in the spectrometer about an axis perpendicular to $\mathbf{B}_0$. The experimental geometry and definition of θ_m are given in figure 2. The director orientation with respect to the cell is described by the angles θ_d and Φ_d. From symmetry considerations we can assume that the angles Φ_d are randomly distributed as long as $\theta_m = 0°$. The relationship between θ_d, Φ_d, θ_m and θ is

$$\cos\theta = \cos\theta_d \cos\theta_m + \sin\theta_d \sin\theta_m \cos\Phi_d. \quad (7)$$

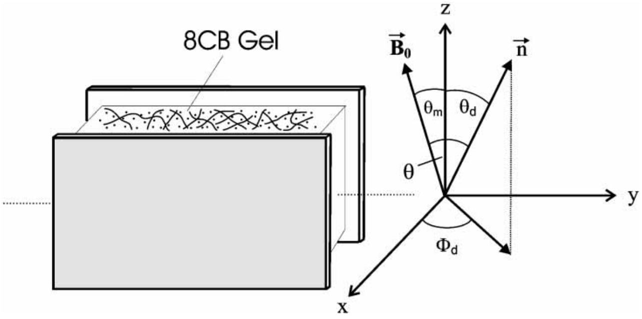

Figure 2. Sample geometry in the spectrometer and the definition of angles θ_d, Φ_d, θ_m and θ.

4. Results and discussion

4.1. *Optical characterization*

Optical investigations on samples containing different amounts of gelator show that the nematic phase transitions are not significantly changed and that the LC texture is unchanged in the gel within the nematic phase when the temperature is varied; see figure 3 (*a*) for

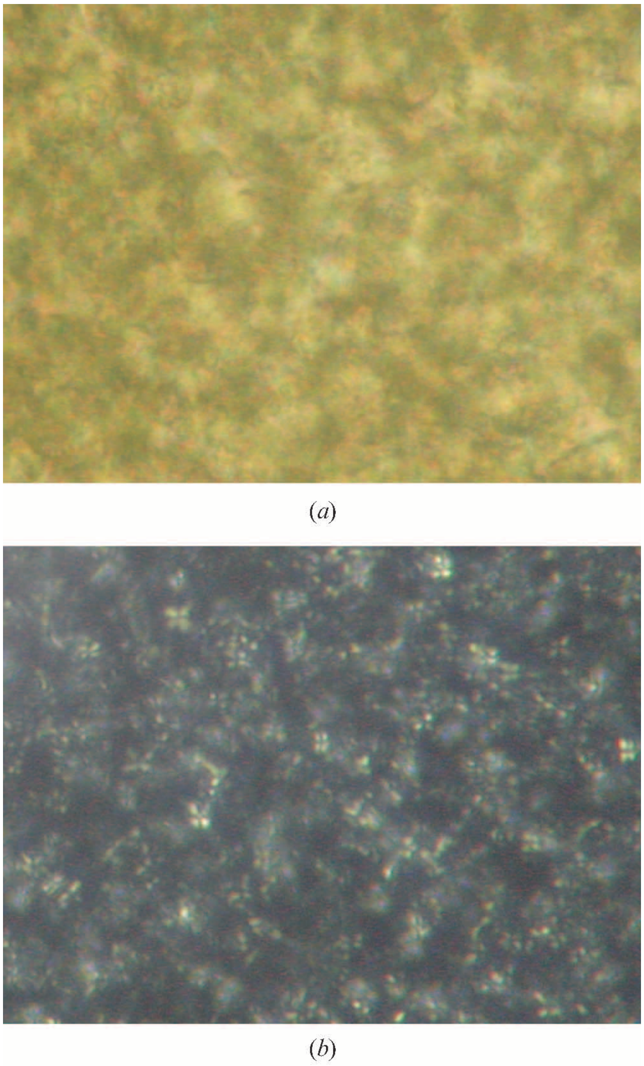
(*a*)

(*b*)

Figure 3. Optical textures of a physical 8CB gel containing 3.0 wt% gelling agent under crossed polarizers. (*a*) $T = 36°C$ (nematic phase): highly birefringent, multidomain pattern; (*b*) $T = 42°C$ (isotropic phase): partially isotropic but with remaining birefringent domains, image size 225 × 169 µm^2.

the 3.0% sample. The cells are highly scattering in the nematic region even after exposure to external magnetic fields (>2 T). They become transparent only in the isotropic phase of 8CB. However, a residual birefringence in the isotropic phase is observed under crossed polarizers in the microscope figure 3 (*b*). This has already been reported for a similar (chemically gelled) system by Hikmet [1]. A simple explanation for these optical effects which is supported later by the NMR investigations, is that the gel network topology is similar to a random orientation. The gel network is formed in the isotropic phase. The birefringence in the isotropic phase in the vicinity of the clearing point indicates the existence of some order, probably a local anisotropy of the gelator crystallite structures, because the residual birefringence only vanishes at about 10 K above the N–I phase transition. There may be an additional contribution from the surface-induced ordering of the mesogens in the close vicinity of the clearing point. The major contribution, however, persisting several degrees above the clearing point, must be attributed to the gelator. At temperatures above 50°C the residual birefringence disappears. We interpret this as the dissolution of the gel network. Above 50°C, the sample behaves optically as well as in the NMR studies in a similar fashion to the pure isotropic 8CB sample.

After cooling the gel that has formed at 50°C into the nematic phase, the sample orientation is influenced by the network. The director is pinned to the gel network and a disordered, multidomain state is formed, with a large defect density induced by the gel network. We assume from the optical appearance that the network structure contains gelator-rich strands, i.e. aggregates of hydrogen bond-bridged gelator fibrils [5, 11, 12], and intermediate regions of essentially pure nematic material. The residual birefringence observed above the bulk clearing point but below the gelation point originates presumably from nematic material encapsulated by the gelator aggregates.

Due to the nematic curvature elasticity, the director alignment in these regions is fixed by the interactions with the network. An applied external magnetic (or electric) field of sufficient strength may reorient the director field, leaving the hydrogen-bonded network intact. A measure of the field strength is the ratio of the magnetic correlation length $\xi_{\mathrm{mag}} = \left[K\pi^2\mu_0/\left(\chi_{\mathrm{a}}\mathbf{B}_0^2\right)\right]^{\frac{1}{2}}$ to the average distance between the hydrogen bonded network strands. The material parameters K and χ_{a} describe an average elastic constant of the nematic and the diamagnetic susceptibility anisotropy, respectively. The latter has its origin in the anisotropic diamagnetic contributions of the biphenyl groups in the 8CB molecular core. In 8CB, χ_{a} is positive, i.e. the director tends to align in the magnetic field direction. In the NMR field used here of the order of 2.3 T, the correlation length is approximately 2 μm (the equation used strictly holds only for a one-dimensional magnetically induced deformation near a planar wall; for the present geometry it is a rather crude approximation, but which gives, at least, the correct order of magnitude). If ξ_{mag} is of the same order of magnitude or smaller than the average distance between the hydrogen-bonded network meshes, the field may distort the director field in the cavities of the network. Apparently, it does not destroy the network skeleton. Otherwise, the samples would gradually align completely along the magnetic field direction, resulting in line shapes similar to those seen for the pure 8CB phase.

The visible light scattering in the nematic phase is caused by the large number of defects in the director field due to the random orientation of the gel network. This is in contrast with samples in which the gel network is created in the ordered phase, i.e. where the gelation temperature is below the clearing point of the mesogen (see, for example, [12], where the same gelator has been mixed with a smectogen). In that case, an oriented gel may be created if the nematic phase is oriented before gelation.

The scattering intensity is enhanced by increased gel former content. The observation that this phenomena becomes more apparent with increasing amount of gel former in 8CB confirms the role of the network. We note that a solution of non-gelating additives in the nematic would usually lead to a *reduction* of nematic order, resulting in the opposite optical effect. In that case, a reduced birefringence with increasing content of the additive would be observed in the nematic phase, and neither scattering nor birefringence would be induced in the isotropic phase. It was observed in thin free-standing smectic gel films that the mesh size of the network decreases with increasing gel former content [12]. We assume that this is also true in the nematic gel in sandwich cells. However, due to the 3D structure it is impossible to identify the network meshes directly in the polarizing microscope.

4.2. ^{1}*H NMR*

In the isotropic phase, two narrow lines corresponding to aromatic and aliphatic protons, are found, figure 4 (*b*), their splitting is of the order of ≈6 ppm. Near the transition to the isotropic phase, the spectra possess a sharp central line that corresponds to isotropic domains in a biphasic region. In the nematic phase, the spectra broaden to a width of *c.* 10 kHz, the central part corresponds to the alkyl chain protons with partially motion-averaged dipolar interactions, while the core protons contribute basically to the wings of the spectra. The assignment of the maxima of the wings to the *ortho*-protons splitting yields a reasonable order parameter in agreement with known literature data, see for example [21]. Typical NMR spectra of pure 8CB are shown in figure 4 (*a*). The isotropic temperature spectrum has been omitted here. Figure 4 (*b*) shows the ^{1}H NMR spectra in the same temperature range for an 8CB sample with 5.0% gelator, recorded during cooling.

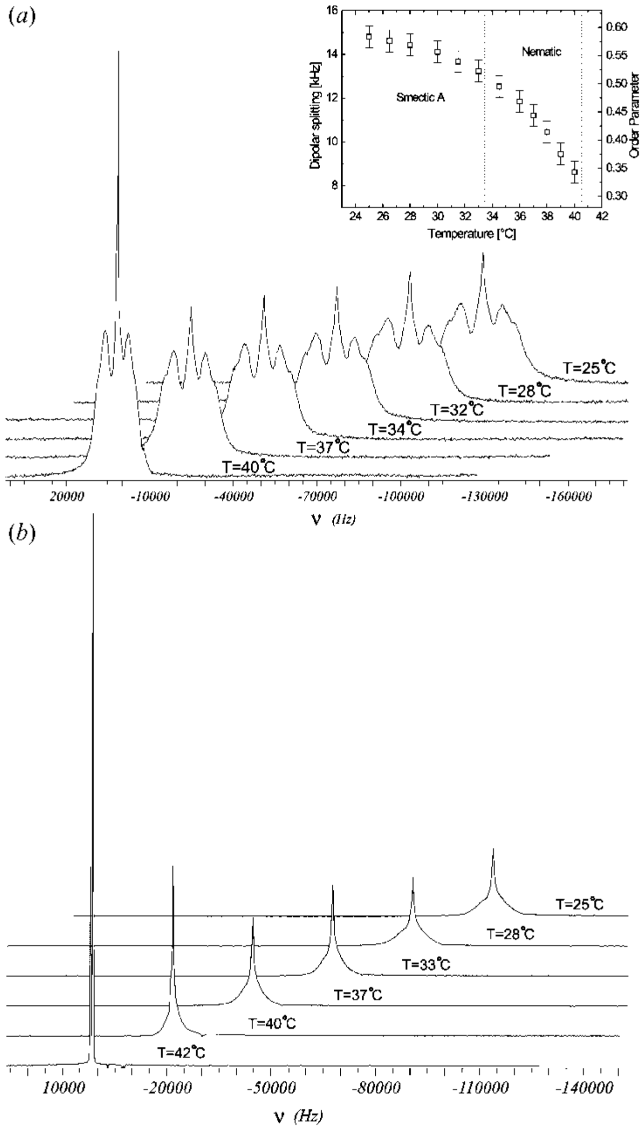

Figure 4. (*a*) Selection of proton NMR spectra of pure 8CB at variable temperatures. The line shape of the perfectly oriented sample scales according to equation (1). In the vicinity of the clearing point, the narrow central line indicates the presence of an isotropic contribution. Above the clearing point, the line collapses to two narrow peaks. The insert gives the temperature dependence of the ^1H NMR dipolar splitting and order parameter for the pure 8CB samples derived from that splitting. (*b*) Selection of proton NMR spectra of 8CB with 5.0 wt% gelator for various temperatures. The line shape corresponds to a random powder pattern, its width scales with the order parameter of 8CB.

The order parameter S has been determined from the proton NMR spectra, using equation (3). The insert of figure 4 shows the temperature dependence of the dipolar splitting and order parameter of pure 8CB. Since we cannot distinguish between the influence of the two prefactors in equation (1), it is not easy to distinguish between the effects of a reduced order parameter and a poor alignment of the sample. We assume therefore in the line shape simulations that the order parameter is unchanged with respect to the pure material. This cannot be proved in the low percentage samples. However, the 5.0% sample line shape can be fit excellently with the model of a spherical powder pattern of the same order parameter (see later) as the pure material. This supports the assumption that the order parameter changes due to addition of gelator are negligibly small for the NMR line shape analysis. Presumably, most of the gelator is contained in the network strands after gelation, so that the material contained in the meshes of the network (the volume between the network strands) is very close to being pure 8CB.

After a discussion of the order parameter, we consider the director orientation in the LC gel which can be obtained from the simulation of the line shape of the proton NMR spectra. In the pure 8CB samples, of course, the alignment in the magnetic field is complete and the temperature-dependent spectra are simply scaled by the order parameter S, whereas $S_\theta \equiv 1$. When pure 8CB samples are rotated into another position in the magnetic field, the director realigns immediately to $\theta = 0°$.

In the gel experiments, we recorded the spectra at different rotation angles θ_m. It is found that the experimental line shapes are almost equivalent in all orientations, independent of θ_m. This is as expected for a nematic phase in a random gel state; no preferential orientation should exist. In the case of the sample containing a lower concentration of gel former, the LC director with positive diamagnetic anisotropy tends to align partially towards the magnetic field $\mathbf{B}_0$. The coherence length ξ_{mag} is obviously smaller than the average dimension of the hydrogen-bonded network meshes. Therefore, the influence of the network is insufficient to fix the director field far from the network strands. The line shape and splitting positions correspond to the director orientation close to $\theta = 0°$, independent of sample rotation. That is, the director is presumably fixed at the gel network but otherwise it is largely distorted towards the magnetic field as illustrated in figure 5 (*b*). When the gelator concentration

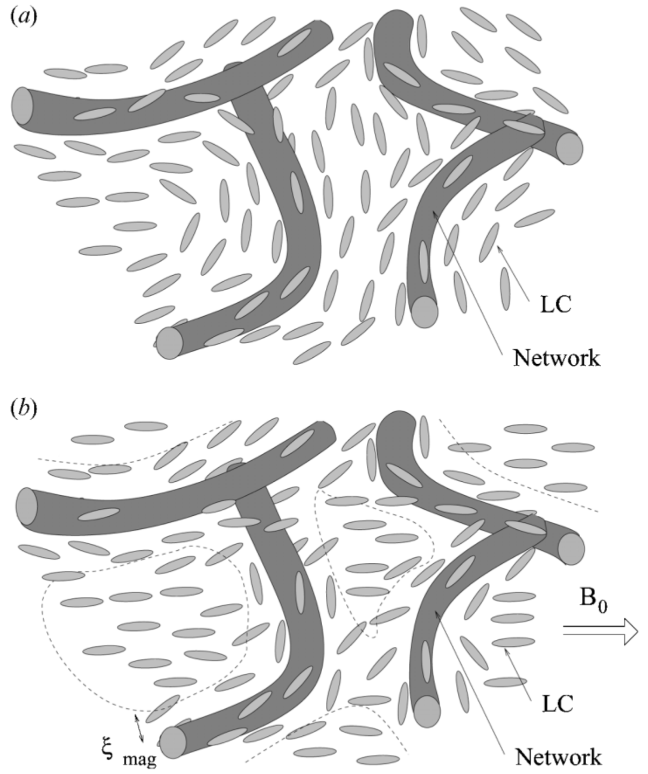

Figure 5. (*a*) Field-free state: the random LC director field is imposed by the interactions between LC mesogens and gel network. The tubes symbolize aggregates of gelator fibrils—as in figure 8 (*c*) of [10]. (*b*) Under a sufficiently strong external magnetic field, the LC director reorients towards the field. In the vicinity of the network strands (within approximately ξ_{mag}, sketched by dashed lines), the original orientation is retained. If the network is sufficiently tight such that ξ_{mag} is comparable to the interfibre distances, the director field remains largely unaffected by the field.

becomes larger (≈3.0%), the influence of the network is strengthened and the reorientation of the director along the field direction is incomplete. At least part of the sample is pinned at the gel network. The director distribution becomes much closer to random distribution. When the sample is rotated in the magnetic field, parts of the director field realign in the new direction, but the overall distribution remains the same. Moreover, no relaxation of the line shape towards that of an oriented sample is observed during the measurements, i.e. the gel network remains stable. At 5.0% concentration, we find that the line shape is in very good agreement with the assumption of a random isotropic powder. In that case, the gel network mesh size has become smaller than the magnetic coherence length, and the director remains almost unaffected by the NMR field, as shown in figure 5 (*a*).

Since in all cases the line shape is independent of the sample orientation, only the 0° spectra have been shown in figures 4 and 6. Figure 6 shows line shapes of the LC gel in the nematic phase with different concentration of gelling agent. A prominent feature of all the spectra is the increased intensity close to the central peak. This peak arises from unoriented parts of the sample, which are already present in the 1.0% sample.

In order to obtain a quantitative picture of the director distribution in the system, we have simulated proton NMR line shapes according to equations (4 and 5) by varying the distribution $n(\theta)$, and by using $f_0(v)$ determined from the $\theta = 0^\circ$ spectra of the pure material with a known order parameter. In the absence of external fields, we know the exact director distribution density $n(\theta_{\text{d}}) = \sin\theta$, is independent of Φ_{d} in the case of a random distribution. The computer simulated line shapes that provide the best approximation to the experimental data, see figures 6 a–c, are shown in figures 6 d–f. The associated director distributions $n(\theta)$ are shown in figure 7. Since the influence of $n(\theta)$ is insufficiently specific to extract $n(\theta)$ unambiguously from a deconvolution of the spectra, model distributions have been constructed. Each of the fits assumes that the director field consists of a randomly disordered part

$$n_{\text{dis}} = n_{\text{dis}}^{(0)} \sin\theta \tag{8}$$

and a part that is partially ordered, i.e. Boltzmann-distributed with respect to the magnetic field direction

$$n_{\text{ord}} = n_{\text{ord}}^{(0)} \sin\theta \exp\left(-A\cos^2\theta\right) \tag{9}$$

where A determines the degree of macroscopic alignment. $A = 0$ corresponds to the randomly disordered state, while with increasing A the distribution focuses towards small angles θ. This rather crude model does not reflect the actual distribution in the intermediate concentration range of gelator, but in the limiting cases of strong network influence (5.0% sample, random powder) and weak network influence (1.0% sample, almost aligned sample) the agreement with the spectra seems rather satisfactory.

One can observe the influence of different gel contents on the LC director orientation in the samples directly from the $n(\theta)$ graphs. Furthermore, the influence of the magnetic field on the orientation of LC gel samples suggests that the director orientation is elastically distorted by the $\mathbf{B}_0$ field but remains fixed at the network skeleton. At low gel former concentration, an external magnetic field can easily align the nematic director field (see the results of the 1.0% sample); on increasing the concentration of the gelator above a critical concentration (nearly ≈3.0%), the average distance between neighbouring network strings or

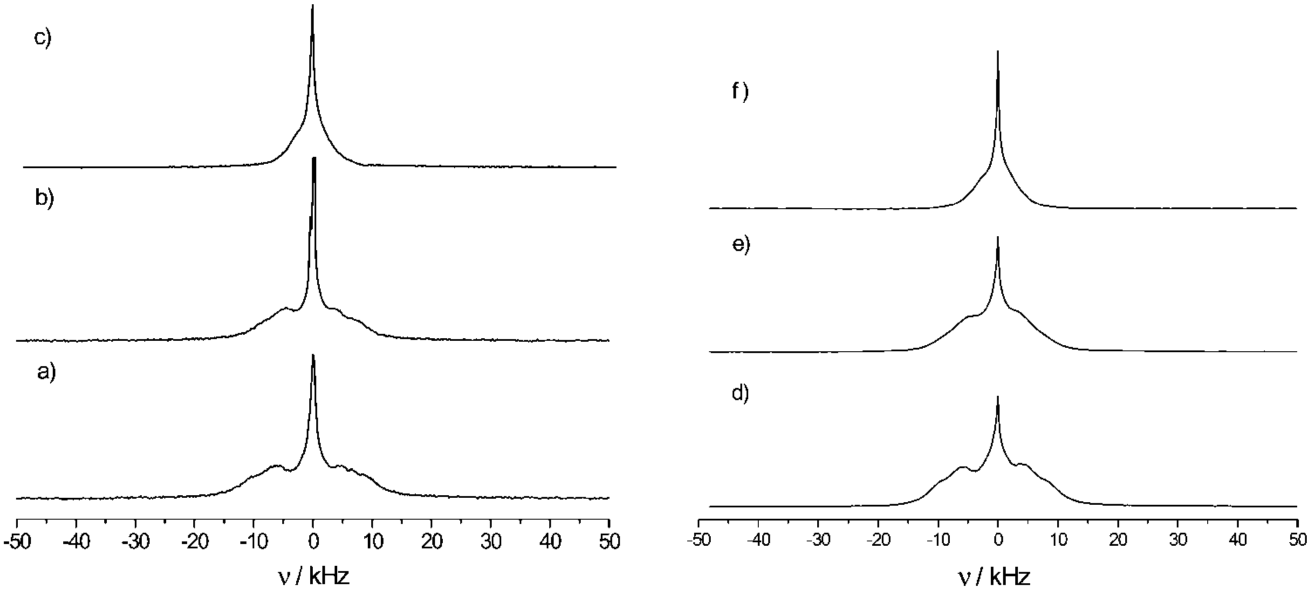

Figure 6. Measured proton NMR line shapes ($\theta_m = 0°$) of 8CB gel at 37°C (nematic phase) with different concentrations of gelling agent. a) 1.0, b) 3.0, c) 5.0 wt.%. Calculated ^{1}H NMR spectra d–f) correspond to the experimental spectra a–c), respectively. The corresponding director distribution densities $n(\theta)$ are shown in figure 7.

clusters becomes smaller than the correlation length corresponding to the magnetic field strength. Since the network is formed in the isotropic liquid and subsequently a random gel structure is obtained in the sample, the major part of the director field remains fixed to the field-free state. The director orientation is very close to the random distribution $n(\theta) = \sin\theta$, even at the 2.34 T $\mathbf{B}_0$ field, as shown in figure 7c.

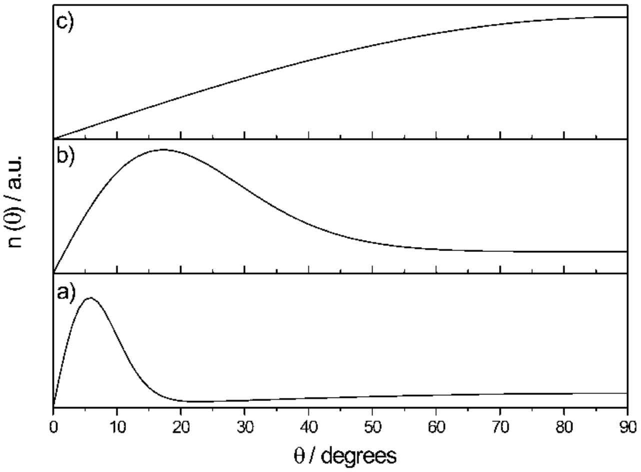

Figure 7. Distribution densities of the angles θ used in the simulation of the spectra shown in figure 6 a–c). The distributions have been generated with equations (8) and (9) with parameters A as a) 50, b) 5, c) 0 and the ratio of $n^{(0)}_{\mathrm{dis}} / n^{(0)}_{\mathrm{ord}}$ as a) 0.003, b) 0.01, c) arbitrary.

5. Conclusions

In this paper we have shown that the proton NMR spectra of a hydrogen-bonded LC gel provide information about order and orientation of the nematic director in these new materials. Our results show that small percentages of hydrogen-bonded gel network are sufficient to stabilize the nematic director even in the strong external magnetic field of the spectrometer. A powder pattern has been obtained in the system as the gel network is formed in the isotropic phase. The critical amount of the gelling agent that is necessary to fix the director orientations is above 3.0%. At lower concentrations, the 2.34 T magnetic field distorts the LC director field, while the gel network structure retains a random orientation memory. With increasing gelator concentration, the disordered director orientation is reinforced. 5.0% gelator is found to be sufficient for a complete stabilization of the director configuration in the NMR field. From the NMR spectra, there are no apparent differences between the nematic and smectic gel states (which, of course, would be expected, for example, in X-ray measurements). The order parameter of the 8CB in the gel is not changed significantly from that of the pure mesogen. The remaining birefringence of the sample above the clearing point is probably caused by the anisotropic structure of the gel network, and vanishes above the gelation point of 50°C.

The authors are much indebted to Christian Tolksdorf and Rudolf Zentel for synthesizing the gelator material, and acknowledge financial support within Sta 425/14 and Ge 718/7-1. We are grateful to J. Rauchfuß and J. Reinmuth for technical support.

References

[1] HIKMET, R. A. M., 1990, *J. appl. Phys.*, **68,** 4406; HIKMET, R. A. M., 1991, *Liq. Cryst.*, **9,** 405; YANG, D. K., CHIEN, L. C., and DOANE, J. W., 1992, *Appl. Phys. Lett.*, **60,** 3102.

[2] LI, J., WANG, Z., CAI, Y., and HUANG, X., 1998, *Ferroelectrics*, **213,** 91; LI, J., ZHAO, W., MA, K., and Huang, X., 1998, *Mol. Cryst. liq. Cryst.*, **321,** 395; LI, J., ZHU, X., XUAN, L., and HUANG, X., 2002, *Ferroelectrics*, **277,** 85.

[3] MATSUYAMA, A., and KATO, T., 2001, *Phys. Rev. E*, **64,** 010701; MATSOYAMA, A., and KATO, T., 2001, *J. chem. Phys.*, **114,** 3817; MATSOYAMA, A., and KATO, T., 2002, *J. chem. Phys.*, **116,** 8175.

[4] KATO, T., 2002, *Science*, **295,** 2414.

[5] KATO, T., KUTSUNA, T., HANABUSA, K., and UKON, M., 1998, *Adv. Mater.*, **10,** 606.

[6] ABDALLAH, D. J., and WEISS, R. G., 2000, *Adv. Mater.*, **12,** 1237.

[7] OYA, M., MACHIDA, S., HORIE, K., KATO, T., and HANABUSA, K., 2000, *Polym. adv. Techn.*, **11,** 456.

[8] MIZOSHITA, N., SUZUKI, Y., KISHIMOTO, K., HANABUSA, K., and KATO, T., 2002, *J. mater. Chem.*, **12,** 2197.

[9] MIZOSHITA, N., HANABUSA, K., and KATO, T., 2003, *Adv. funct. Mater.*, **13,** 313.

[10] ABE, H., KIKUCHI, H., KAJIYAMA, T., HANABUSA, K., and KATO, T., 2002, *Liq. Cryst.*, **29,** 1503.

[11] TOLKSDORF, C., and ZENTEL, R., 2001, *Adv. Mater.*, **13,** 1307.

[12] LI, J., STANNARIUS, R., TOLKSDORF, C., and ZENTEL, R., 2003, *Phys. Chem. chem. Phys*, **5,** 916.

[13] PRIGANN, J., TOLKSDORF, C., SKUPIN, H., ZENTEL, R., and KREMER, F., 2002, *Macromolecules*, **35,** 4150.

[14] MIZOSHITA, N., SUZUKI, Y., HANABUSA, K., and KATO, T., 2002, in *Abstracts of the 19th ILCC*, Edinburgh, UK, p. 430.

[15] GOLEMME, A., ZUMER, S., ALLENDER, D. W., and DOANE, J. W., 1988, *Phys. Rev. Lett.*, **61,** 2937.

[16] STANNARIUS, R., CRAWFORD, G. P., CHIEN, L. C., and DOANE, J. W., 1991, *J. appl. Phys.*, **70,** 135.

[17] BERGGREN, E., ZANNONI, C., CHICCOLI, C., PASINI, P., and SEMERIA, F., 1994, *Phys. Rev. E*, **49,** 2929.

[18] SCHMIEDEL, H., HILLNER, B., GRANDE, S., LÖSCHE, A., and LIMMER, ST., 1980, *J. magn. Res.*, **40,** 369.

[19] LIMMER, S., SCHMIEDEL, H., HILLNER, B., LÖSCHE, A., and GRANDE, S., 1980, *J. Physique*, **41,** 869.

[20] DONG, R. Y., 1994, *Nuclear Magnetic Resonance of Liquid Crystals* (New York: Springer).

[21] SHERRELL, P. L., and CRELLIN, D. A., 1979, *J. Physique*, **40,** 211.